

Full Terms & Conditions of access and use can be found at
<http://www.tandfonline.com/action/journalInformation?journalCode=gmcl20>



Synthesis, spectral, X-ray diffraction and DFT studies on 1-(2-methyl-2-propenyl)-3-(2,3,4,5,6-pentamethylbenzyl) benzimidazolium chloride hydrate

Neslihan Şahin^{a,b,c}, Işın Kılıç-Cıkla^d, Namık Özdemir^e, Nevin Gürbüz^{b,c}, and İsmail Özdemir^{b,c}

^aDepartment of Basic Education, Faculty of Education, Cumhuriyet University, Sivas, Turkey; ^bDepartment of Chemistry, Faculty of Science and Art, İnönü University, Malatya, Turkey; ^cCatalysis Research and Application Center, İnönü University, Malatya, Turkey; ^dDepartment of General Secretary, Ondokuz Mayıs University, Samsun, Turkey; ^eDepartment of Mathematics and Science Education, Faculty of Education, Ondokuz Mayıs University, Samsun, Turkey

ABSTRACT

A new benzimidazole based N-heterocyclic carbene (NHC) salt (**1**) was synthesized by the reaction of benzimidazole precursor with alkyl halide. The structure of **1** was determined by elemental analysis, FT-IR, ¹H NMR and ¹³C NMR spectroscopy techniques and X-ray crystallography. The compound crystallized in the triclinic space group *P*-1 with two molecules in the unit cell. The optimization of **1** was firstly performed at B3LYP/6-311G++(d,p) level, then the theoretical spectral studies performed and compared with the experimental values. Besides the frontier molecular orbital energies and chemical reactivity analysis of **1**, together with the electrostatic potential and molecular electrostatic potential analyses were performed at the same level of theory.



KEYWORDS

DFT calculations;
N-Heterocyclic carbene; X-ray diffraction; ¹H and ¹³C NMR

1. Introduction

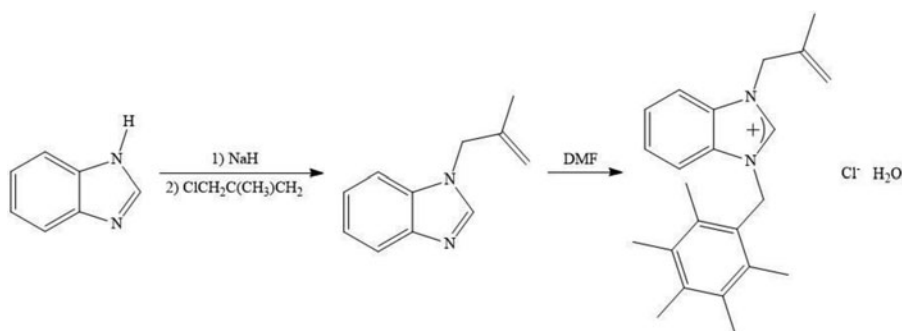
N-Heterocyclic carbene (NHC) is a cyclic carbene species with two neighboring nitrogen atoms. NHCs were first searched out in 1968 by Ofele, Wanzlick and Schonherr [1, 2]. In the 1970's, Lappert submitted a series of complexes via cleavage of the electronically rich olefin [3]. In 1991, the first isolated NHC was reported by Arduengo [4]. The synthetic process is deprotonation of precursor azolium salt with sodium or potassium hydride in the presence of KOTBu in DMSO [5–7]. Another developed method is based on deprotonation of the corresponding salts in liquid ammonia [8, 9]. Reaction of imidazol-2-thiones with potassium metal [10], thermal elimination of methanol from adducts to form triazol-2-ylidene [11], and elimination of phenoxides is other synthesis methods.

Recently, N-heterocyclic carbenes have been increasingly used as ligands in coordination chemistry due to their strong electron-donating property. Moreover, NHCs have excellent air and moisture stability [12]. N-Heterocyclic carbenes have been used in metal complex catalysts for many important organic synthesis reactions such as hydrogenation [13], hydroformylation [14, 15], C-C coupling [16, 17], olefin metathesis [18, 19], hydrosilylation

CONTACT Işın Kılıç-Cıkla  ikilic@omu.edu.tr  Department of General Secretary, Ondokuz Mayıs University, Samsun 55139, Turkey.

Color versions of one or more of the figures in the article can be found online at www.tandfonline.com/gmcl.

© 2018 Taylor and Francis Group, LLC



Scheme 1. Synthesis of **1**.

[20, 21] and etc. in pharmaceutical sciences [22, 23]. Also, recent studies have employed the use of NHC ligands in order to reduce carbon dioxide into either methanol or formic acid [24–27].

We herein report preparation, detailed X-ray structural analysis, spectroscopic characterization and some theoretical properties of newly synthesized 1-(2-methyl-2-propenyl)-3-(2,3,4,5,6-pentamethylbenzyl) benzimidazolium chloride hydrate molecule.

2. Materials and measurements

2.1. Synthesis

Benzimidazole (10 mol) was added to a solution of NaH (10 mol) in dry THF (30 mL), and the mixture was stirred for 1 h at room temperature. 3-Chloro-2-methyl-1-propene (10.1 mol) was added dropwise upon to obtained solution and heated for 24 h at 60°C. Then, the THF was removed under the vacuum. Dichloromethane (50 mL) was added upon the solid. The mixture was filtered and the obtained clear solution was concentrated under vacuum. Then the solution was distilled. The obtained 1-(2-methyl-2-propenyl)benzimidazole (1 mmol) and 2,3,4,5,6-pentamethylbenzyl chloride (1 mmol) were stirred in DMF (5 mL) for 24 h at 80°C. White products were collapsed. Following the completion of the process, the solution was filtered, and rinsed out with diethylether and dried under vacuum. Crude product was recrystallized from dichloromethane/diethylether mixture (Scheme 1).

2.2. Experimental details

The synthesis of **1** was carried out under argon in flame-dried glassware using standard Schlenk line techniques. Chemicals and solvents were purchased from Sigma Aldrich Co. (Dorset, UK). The solvents used were dried by distillation over the drying agents and were transferred under Argon. Elemental analyses were performed by the Turkish Research Council (Ankara, Turkey) Microlab. Melting point was determined using Electrothermal 9100 melting point detection apparatus.¹H NMR and ¹³C NMR spectra were recorded using a Varian As 400 Mercury spectrometer operating at 400 MHz (¹H), 100 MHz (¹³C) in CDCl₃ with tetramethylsilane as the internal reference. Yield: 84%, mp 201–202°C, $\nu(\text{CN})$: 1556 cm⁻¹. ¹H NMR (399.9 MHz, CDCl₃) δ (ppm): 1.75 (s, 3H, NCH₂C(CH₃)CH₂), 2.29, 2.27 and 2.24 (s, 15H, CH₂C₆(CH₃)₅-2,3,4,5,6), 2.49 (border s, 2H, H₂O), 4.85 (s, 1H, NCH₂C(CH₃)CH₂), 5.06 (s, 1H, NCH₂C(CH₃)CH₂), 5.36 (s, 2H, NCH₂C(CH₃)CH₂), 5.87 (s, 2H, CH₂C₆(CH₃)₅-2,3,4,5,6), 7.33–7.29 (m, 2H, NC₆H₄N), 7.57–7.47 (m, 1H,

Table 1. Crystallographic data of **1**.

CCDC deposition number 1582192			
Crystal data		Data collection	
Chemical formula	C ₂₃ H ₂₉ N ₂ .Cl.H ₂ O	Diffractometer	STOE IPDS2
Color/ shape	Colorless/ Prism	Reflections collected	18790
Formula weight	386.95	Independent/observed refl.	4959/2484
Crystal size (mm)	0.68 × 0.34 × 0.13	Absorption correction	integration
Wavelength (Å)	MoK _α , λ = 0.71073	<i>T</i> _{min} , <i>T</i> _{max}	0.9094, 0.9790
Temperature (K)	296	<i>F</i> ₀₀₀	416
Crystal system	Triclinic	<i>R</i> _{int}	0.087
Space group	<i>P</i> -1	θ range (°)	1.69 ≤ θ ≤ 27.62
Unit cell parameters		Index ranges	−11 ≤ <i>h</i> ≤ 11, −13 ≤ <i>k</i> ≤ 13, −16 ≤ <i>l</i> ≤ 16
<i>a</i> , <i>b</i> , <i>c</i> (Å)	9.0007(10), 10.0321(11), 12.7255(15)	Refinement	
α, β, γ (°)	77.665(9), 73.502(9), 81.473(9)	Data/restraints/parameters	4959/3/255
Volume (Å ³)	1071.6(2)	Goodness of fit on <i>F</i> ²	1.026
<i>Z</i>	2	Final <i>R</i> indices [<i>I</i> > 2σ(<i>I</i>)]	0.0695, 0.1796
Density (Mgm ^{−3})	1.199	Δρ _{max} , Δρ _{min} (e/Å ³)	0.23, −0.18
μ (mm ^{−1})	0.193		

NC₆H₄N), 7.84 (d, 1H, NC₆H₄N, *J* = 7.6 Hz), 11.04 (s, 1H, NCHN). ¹³C NMR (100.5 MHz, CDCl₃) δ (ppm): 17.1 (CH₂C₆(CH₃)₅-2,3,4,5,6), 19.7 NCH₂C(CH₃)CH₂), 48.4 (CH₂C₆(CH₃)₅-2,3,4,5,6), 53.5 (NCH₂C(CH₃)CH₂), 113.7 (NCH₂C(CH₃)CH₂), 115.3 (NCH₂C(CH₃)CH₂), 124.9, 127.0, 127.1, 131.5, 131.8, 133.6, 134.0, 137.4 and 137.8 (NC₆H₄N and CH₂C₆(CH₃)₅-2,3,4,5,6), 143.8 (NCHN). % Anal. Calcd. for C₂₃H₂₉N₂.Cl.H₂O: C, 71.39; H, 8.08; N: 7.24. Found: C, 71.41; H, 8.10; N, 7.26.

2.3. X-ray crystallography

Crystallographic measurements were carried out on STOE IPDS II diffractometer using MoK_α radiation (λ = 0.71073 Å). The structure was solved by direct methods using SHELXT-2016 [28] and refined by a full matrix least squares procedure using SHELXL-2017 [29]. All H atoms were placed in geometrically idealized positions and constrained to ride on their parent atoms with C–H distances in the range 0.93–0.97 Å. The DFIX restraints of O–H = 0.82 Å and H–H = 1.35 Å were applied for OH₂ distances. The final period of refinement process results in *R*₁ = 0.0695 and *wR*₂ = 0.1796 for the observed reflections. A summary of the crystal data and refinement parameters of the compound are listed in Table 1. Molecular figures were generated using PLATON [30] and ORTEP-3 [31].

2.4. Computational details

In the present work, all theoretical calculations were performed using the Gaussian09W program [32]. The first-hand geometry of the compound was taken from the X-ray diffraction results. Geometry optimization was firstly performed using the density functional theory with B3LYP. The 6–311++(d,p) basis set was assigned to all atoms. Vibrational wavenumbers were computed at same DFT level and no imaginary wavenumber modes were obtained. A scaling factor of 0.9679 [33] was applied to obtain a better agreement between the optimized and experimental wavenumbers. The ¹H and ¹³C NMR chemical shifts were calculated within the GIAO approach [34] and converted to the TMS scale. The default solvation model

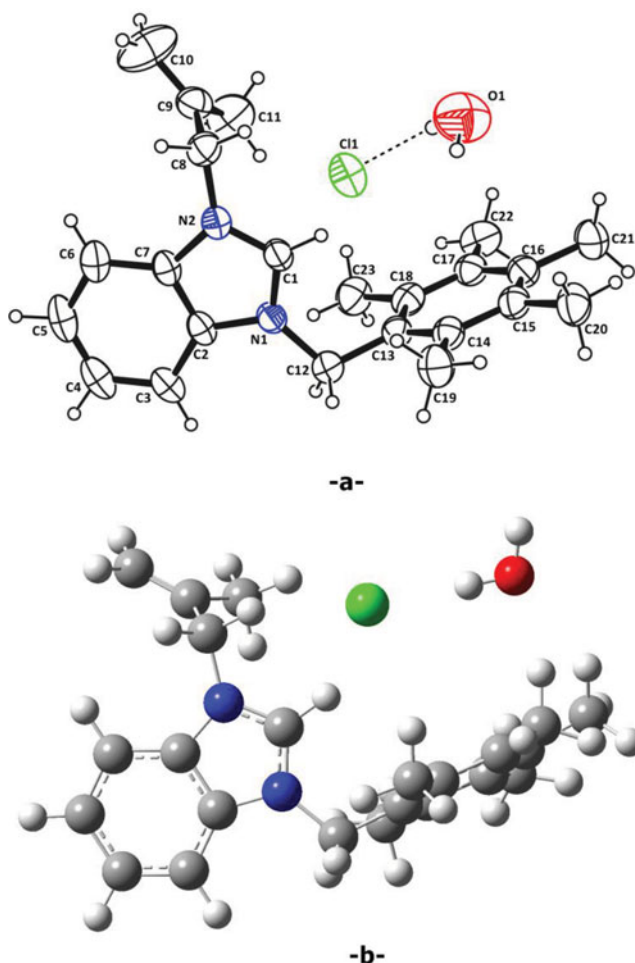


Figure 1. (a) The molecular structure of **1** with thermal ellipsoids at 50% probability. Dashed lines show the intermolecular O–H...Cl hydrogen bond. (b) The optimized geometry of the compound obtained at B3LYP/6-311G++(d,p) level.

IEF-PCM [35] was preferred to include the effect of solvent on the theoretical NMR parameters using chloroform. Since experimental ^1H NMR chemical shift values are not available for individual hydrogen atoms of CH_2 and CH_3 groups, we have presented the average of the computed values for these hydrogen atoms. In order to investigate the reactive sides of **1**, electrostatic potential (ESP) and molecular electrostatic potential (MEP) analyses were performed by B3LYP/6-311G++(d,p) method. We also calculated the HOMO-LUMO energies and chemical reactivity parameters of the compound at the same level of theory.

3. Results and discussion

3.1. Molecular geometry of NHC salt **1**

From the single crystal X-ray diffraction analysis, it can be inferred that NHC salt **1** crystallizes with a water molecule in the asymmetric unit. The experimental and optimized molecular geometries of the title compound are shown in Fig. 1 and selected geometric parameters are given in Table 2.

Table 2. Comparison of some important geometric parameters of **1** with the experimental data.

Parameters Bond lengths(Å)	XRD	DFT 6–311G++(d,p)	Related experimental data
N1–C1	1.323(4)	1.33897	1.310(4) ^a , 1.331(8) ^b , 1.322(4) ^c , 1.345(4) ^d
N2–C1	1.323(4)	1.33933	1.355(4) ^a , 1.335(7) ^b , 1.336(4) ^c , 1.336(4) ^d
N1–C2	1.390(3)	1.39603	1.408(4) ^a , 1.334(8) ^b , 1.396(4) ^c , 1.400(4) ^d
N2–C7	1.389(3)	1.39414	1.394(4) ^a , 1.379(7) ^b , 1.399(4) ^c , 1.391(4) ^d
N1–C12	1.479(4)	1.49100	1.476(4) ^d
N2–C8	1.463(4)	1.58000	1.476(4) ^d
C8–C9	1.493(5)	1.51247	
C9–C10	1.380(6)	1.33431	
C9–C11	1.403(6)	1.50468	
C12–C13	1.514(4)	1.51019	
<i>Bond angles (°)</i>			
N2–C1–N1	111.1(2)	110.09955	111.1(3) ^a , 108.8(6) ^b , 108.9(3) ^d
C1–N1–C2	107.9(2)	110.09955	108.5(3) ^d
C1–N1–C12	126.9(2)	126.47043	
C1–N2–C7	107.9(2)	108.57070	109.4(3) ^d
C1–N2–C8	126.0(2)	124.70954	
N1–C12–C13	112.6(2)	114.08427	
N2–C8–C9	112.1(3)	113.10372	
<i>Torsion angles(°)</i>			
C7–N2–C1–N1	0.4(3)	– 0.14293	
N1–C12–C13–C14	101.2(3)	91.19172	
N1–C12–C13–C18	– 78.9(4)	– 90.58814	
C1–N1–C12–C13	– 25.1(5)	– 22.84535	
C2–N1–C12–C13	154.1(3)	160.29970	
N2–C8–C9–C10	145.0(4)	124.17286	
N2–C8–C9–C11	– 34.6(5)	– 60.01847	

a,b,c,d: Taken from Ref. [35], [36], [37], [38], respectively.

According to X-ray diffraction data, NHC salt **1** crystallized in triclinic space group *P* -1 with two molecules in the unit cell. The benzimidazole ring system is nearly planar with the maximum deviation of 0.022 Å (C2) from mean plane. The N1—C1, N2—C1, N1—C2 and N2—C7 bond distances [1.323(4), 1.323(4), 1.390(3) and 1.389(3) Å, respectively] and C1—N2—C7, C1—N1—C2 and N1—C1—N2 bond angles [107.9(2), 107.9(2) and 111.1(2)°, respectively] are similar to those found in related benzimidazole compounds [36–39]. The pentamethylbenzyl ring plane is almost perpendicular to this plane with an angle of 87.69°. This angle has changed to 79.37° in the optimized geometry. The orientation of the compound changed noticeably with the optimization. In around 2-methyl-2-propenyl chain, while the N2—C8—C9—C10/C11 torsion angles were experimentally observed at 145.0(4)°/-34.6(5)°, computed at 124.17°/-60.01° for B3LYP. The orientation of pentamethylbenzyl ring was defined by torsion angles N1—C12—C13—C14 [101.2(3)°] and C2—N1—C12—C13 [154.1(3)°], but these torsion angles in the optimized structure have been calculated at 91.19° and 160.29°, respectively.

In the molecular structure of 1-(2-methyl-2-propenyl)-3-(2,3,4,5,6-pentamethylbenzyl) benzimidazolium chloride hydrate, the atom O of water molecule acts as hydrogen-bond donor to atom chlorine with the parameters H...Cl = 2.329(12) Å and O-H...Cl = 169°. The intermolecular bond has been calculated more strongly with H...Cl = 2.210 Å and O-H...Cl = 175°. The intermolecular hydrogen bond which formed between the atom C12 in main molecule and the atom O1 in the molecule at (*x*, 1+*y*, *z*) supports the crystal packing of the structure, as seen in Fig. 2. The geometric parameters of these interactions are listed in Table 3. There are also $\pi \cdots \pi$ stacking interactions between the benzimidazole ring systems in the

Table 3. Hydrogen bonding geometry of **1** (Å, °)

D-H...A	D-H	H...A	D...A	D-H...A
O1-H1A...Cl1	0.82(2)	2.329(12)	3.138(4)	169
C12-H12B01 ⁱ	0.97	2.58	3.468(5)	152

D: donor; A: acceptor. Symmetry codes: (i) $x, 1+y, z$

molecules at (x, y, z) and $(1-x, 2-y, -z)$ with the corresponding ring-centroid separations being 3.5334 and 3.5879 Å (Fig. 3).

3.2. Spectroscopic data of NHC salt **1**

The ^{13}C and ^1H NMR spectra of NHC salt **1** in CDCl_3 are shown in Figs. 4–5 and chemical shifts are listed in Table 4 together with the calculated values. ^1H peaks are labeled as singlet (s), doublet (d) and multiplet (m). Chemical shifts and coupling constants are reported in ppm and in Hz, respectively. The isotropic shielding values were used to calculate the isotropic chemical shifts (δ) with respect to TMS [$\delta_{\text{iso}}(\text{X}) = \sigma_{\text{TMS}}(\text{X}) - \sigma_{\text{iso}}(\text{X})$]. The calculated ^1H and

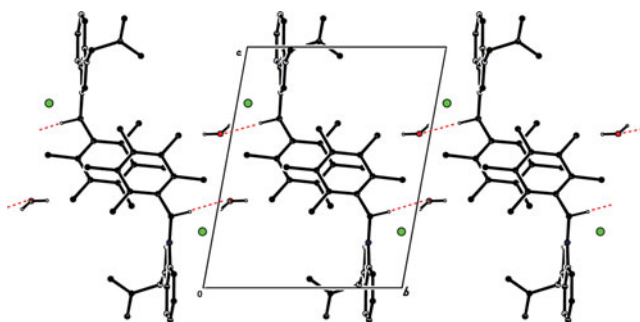


Figure 2. A partial view of the packing of **1**, showing hydrogen bond interactions as red dashed lines (H atoms in hydrogen bonds have only been showed in main molecule).

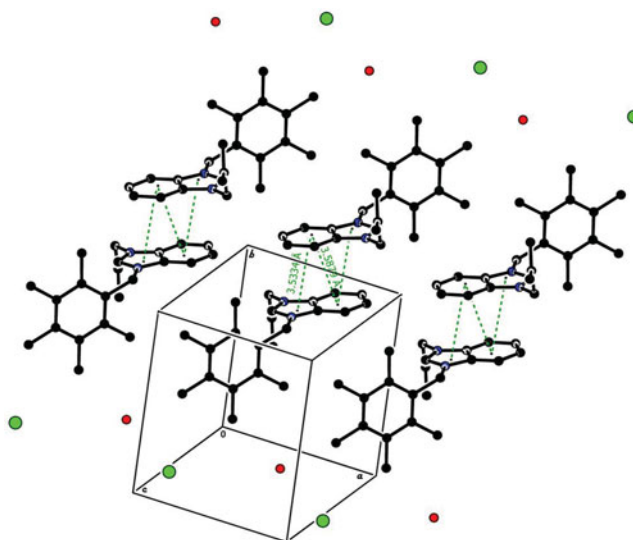


Figure 3. A view of the packing of **1** from c face. Green lines show the π – π interactions between the centres of rings. H atoms have been omitted for clarity.

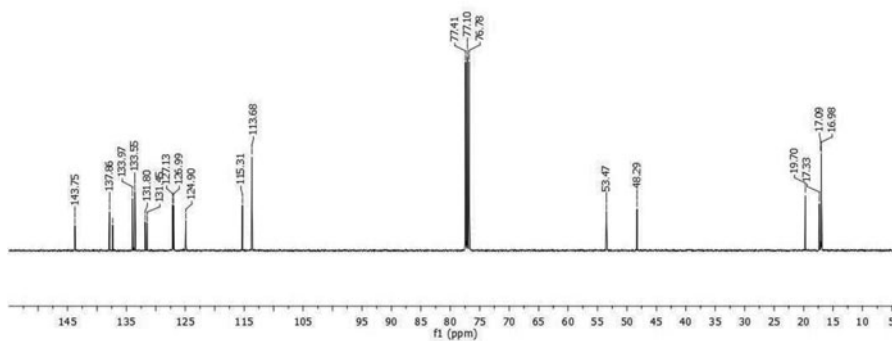


Figure 4. ^{13}C NMR chemical shifts of **1** in CDCl_3 .

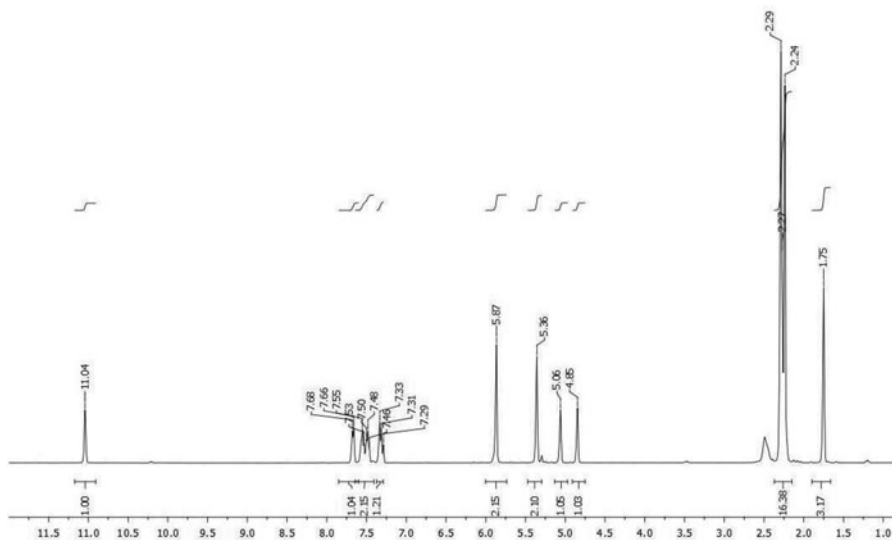


Figure 5. ^1H NMR chemical shifts of **1** in CDCl_3 .

^{13}C chemical shielding of TMS at B3LYP/6-311G++(d,p) level in CDCl_3 are 31.97 ppm and 184.66 ppm, respectively.

The unknown chemical properties of the complicated compounds can be clarified by the isotropic chemical shifts of the elements. The benzimidazolium salt has an acidic NCHN proton which came to at 11.04 ppm as a singlet in the ^1H NMR spectrum. And the chemical shift of the corresponding carbene carbon was appeared at 143.8 ppm in the ^{13}C NMR spectrum. These chemical shifts have duly been calculated at 12.66 ppm and 154.0 ppm in B3LYP. In aromatic rings, the chemical shifts corresponding to carbon and hydrogen atoms are usually observed in the region of 100–160 ppm and 6–8 ppm, respectively [40, 41]. In the present work, aromatic protons on the benzimidazolium ring were appeared at 7.33–7.29, 7.77–7.47 and 7.84 ppm, respectively. Aromatic carbons at the benzimidazolium ring and pentamethylbenzyl were monitored 124.9, 127.0, 127.1, 131.5, 131.8, 133.6, 134.0, 137.4 and 137.8 ppm, respectively. Methyl substituted benzylic proton and carbon were detected at 5.87 ppm as a singlet and 48.4 ppm and calculated 5.51 ppm and 52.1 ppm, respectively. Methyl protons on the benzylic group signaled three different singlet that are 2.24, 2.27 and 2.29 ppm. And carbons of these methyl groups came to 17.0, 17.1 and 17.3 ppm at the ^{13}C NMR spectrum.

Table 4. Experimental and calculated ^1H and ^{13}C NMR chemical shifts $\delta(\text{ppm})$ from TMS.

Atom	Experimental	Calculated	Atom	Experimental	Calculated
H(H_2O)	2.49 s	2.23 ^a	C1	143.8	154.0
H1	11.04 s	12.66	C2	131.8	140.0
H3	7.84 d, $J = 7.6\text{Hz}$	8.08	C3	133.6	118.9
H4	7.47–7.57 m	7.98	C4	134.0	133.8
H5	7.29–7.33 m	7.96	C5	137.4	133.7
H6	7.47–7.57 m	8.04	C6	137.8	120.6
H8(CH_2)	5.36 s	6.12 ^a	C7	143.8	140.8
H10(CH_2)	4.85 s, 5.06 s	5.49 ^a	C8	53.5	59.1
H11(CH_3)	1.75 s	1.68 ^a	C9	115.3	154.8
H12(CH_2)	5.87 s	5.51 ^a	C10	113.7	122.6
H19(CH_3)	2.29 s	2.69 ^a	C11	19.7	19.9
H20(CH_3)	2.27 s	2.58 ^a	C12	48.4	52.1
H21(CH_3)	2.24 s	2.55 ^a	C13	127.0	130.2
H22(CH_3)	2.27 s	2.32 ^a	C14	124.9	143.7
H23(CH_3)	2.29 s	2.21 ^a	C15	127.1	145.9
			C16	127.0	149.1
			C17	124.9	141.3
			C18	127.1	141.8
			C19	17.0	20.2
			C20	17.1	19.0
			C21	17.3	19.5
			C22	17.1	19.3
			C23	17.0	20.0

^a: average (the atom numbering according to Fig. 1 used in the assignment of chemical shifts.)

Theoretical ^1H and ^{13}C chemical shifts of methyl groups on the benzylic group were calculated in the range of 2.21–2.69 ppm and 19.0–20.2 ppm, respectively. In the calculated spectrum, $-\text{CCH}_3$ protons belonging to 2-methyl-2-propenyl which detected at 1.75 ppm shifted to higher field, and NCH_2 protons shifted to higher frequencies. Terminal $-\text{CH}_2$ on the 2-methyl-2-propenyl came to 4.85 and 5.06 ppm as two different singlets. Carbons of 2-methyl-2-propenyl were detected at 53.5, 115.3, 113.7 and 19.7 ppm and calculated at 59.1, 154.8 122.6 and 19.9 ppm, respectively. The recorded chemical shifts of NHC salt **1** are mostly compatible with the calculated values and the previously reported results [42]. Also, protons of water on the NHC salt **1** gave a border singlet at 2.49 ppm.

The experimental and theoretical IR spectra of NHC salt **1** are shown in Fig. 6 and some characteristic vibrations were given in Table 5. The experimental spectrum of the compound contains some characteristic bands of the stretching vibrations of the $\text{C}=\text{N}$, $\text{C}-\text{H}$ and $\text{C}=\text{C}$ groups. Evident of formation of the benzimidazolium salt **1** was $\nu(\text{C}=\text{N})$ bond which showed a peak at 1557 cm^{-1} and calculated at 1522 cm^{-1} . While the stretching vibrations of $\text{C}-\text{H}$ bonds have three or four peaks in the region $3000\text{--}3100\text{ cm}^{-1}$, the $\text{C}=\text{C}$ stretching vibrations usually occur in the region $1400\text{--}1625\text{ cm}^{-1}$ in the literature [43]. Vibrations belonging to the $\text{C}-\text{H}$ aromatic stretching were observed 3069 , 3096 and 3111 cm^{-1} . Aliphatic $\text{C}-\text{H}$ stretching vibrations of methyl group were viewed at 2941 and 2914 cm^{-1} . Peaks at 1609 and 1662 cm^{-1} are $\text{C}=\text{C}$ stretching vibration modes. These peaks were calculated with strong intensity at 1588 and 1652 cm^{-1} . It is known that the OH vibrations of nonhydrogen-bonded or a free hydroxyl group occur strongly in the $3550\text{--}3700\text{ cm}^{-1}$ region. If an intramolecular hydrogen bonding presents, the $\text{O}-\text{H}$ stretching band would reduce to $3200\text{--}3550\text{ cm}^{-1}$ region, due to the sensitivity of the OH group vibrations to the environment [44]. While the nonhydrogen-bonded $\text{O1}-\text{H1B}$ stretching vibration occurs at 3756 cm^{-1} in the calculated spectrum of NHC salt **1**, there is a strong peak at 3407 cm^{-1} corresponding to $\text{O1}-\text{H1A}$ stretching vibration.

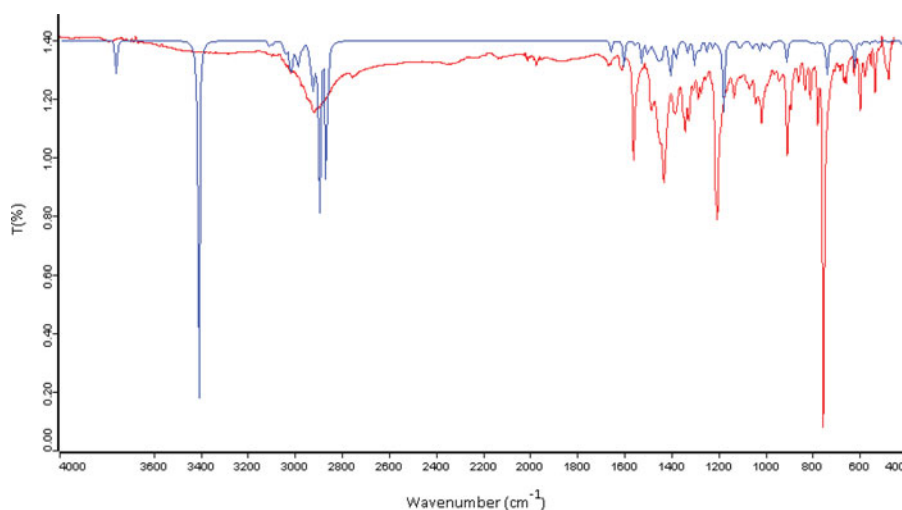


Figure 6. FT-IR spectra belong to experimental (red) and optimized (blue) structures.

3.3. HOMO-LUMO and chemical reactivity analyses

Frontier molecular orbitals which called as HOMO (highest occupied molecular orbital) and LUMO (lowest unoccupied molecular orbital) have an important role in molecular interactions. While the HOMO energy symbolizes the ability of giving an electron, LUMO energy represents the ability of getting an electron. Since the energy gap between these orbitals is closely related to electron conductivity, it is a critical parameter to define the molecular electrical transport [45]. The energy gaps are also liable for the chemical and spectroscopic properties of organic molecules. In order to explain the energetic and chemical reactivity of NHC

Table 5. Some experimental and calculated vibrational frequencies (cm^{-1}) of **1**.

Assignments ^a	KBr	B3LYP/6-311G++(d,p)
ν (O-H)		3756,3407
ν ($\text{C}^{10}\text{-H}_2$) as		3107
ν ($\text{C}^{10}\text{-H}_2$) s		3028
ν ($\text{C}^{\text{aromatic}}\text{-H}$) s	3096–3011	3101
ν ($\text{C}^{\text{aromatic}}\text{-H}$) as		3090
ν (C-H_3) as	2941	3042–2982
ν (C-H_3) s	2914	2931–2912
ν ($\text{C}^{12}\text{-H}_2$) as		3020
ν ($\text{C}^{11}\text{-H}_3$) as		2996
ν ($\text{C}^{11}\text{-H}_3$) s		2919
ν ($\text{C}^8\text{-H}_2$) as		2996
ν ($\text{C}^8\text{-H}_2$) s		2894
ν ($\text{C}^{12}\text{-H}_2$) s		2982
ν (C-H)		2863
ν (C=C)	1609,1662	1588,1652
ν (C=N)	1557	1522
α (O-H)		1598
α (C-H ₂)	1429	1405
γ ($\text{C}^1\text{-H}$)	1204	1174
ω ($\text{C}^{10}\text{-H}_2$)		903
ω (O-H)		618

^a; ν : stretching, γ : rocking, α : scissoring ω : wagging.

^s: symmetric, as: asymmetric.

Table 6. Calculated HOMO-LUMO energies and chemical reactivity descriptors of the compound.

Molecular properties (eV)	Calculated values
HOMO energy, E_{HOMO}	− 5.73
LUMO energy, E_{LUMO}	− 2.11
Energy gap, ΔE	3.62
Ionization potential, IP	5.73
Electron Affinity, EA	2.11
Electronegativity, χ	3.92
Chemical hardness, η	1.81
Chemical potential, μ	− 3.92
Electrophilicity Index, ω	4.24
Global softness, S (eV) ^{−1}	0.55

salt **1**, some characteristics such as hardness (η), chemical potential (μ), softness (S), electronegativity (χ) and electrophilicity index (ω) were calculated using HOMO and LUMO energies. The calculated results are listed in Table 6.

The hardness and softness are decisive criterions to define chemical reactivity or kinetic stability of a molecule. While the soft molecules have small energy gaps, the hard ones have large energy gaps [46]. So it can be said that the hard molecules are more stable than the soft ones. Electronegativity states the ability of an atom or a functional group to pull electrons or electron density towards itself. The energy lowering due to maximal electron flow between HOMO and LUMO orbitals can be evaluated using a factor called as electrophilicity index [47].

The energy and compositions of some selected molecular orbitals are given in Table 7 and the pictorial representations of molecular orbital distributions are shown in Fig. 7. In LUMO, the charge density is mainly localized over the benzimidazole ring with contributions of 97%. Whereas HOMO is fully characterized by a charge distribution on atom chlorine (94%). The calculated energy gap for NHC salt **1** is the medium energy gap which value of 3.62 eV and shows the high electrical activity of the compound.

Table 7. Energy and compositions of some selected molecular orbitals.

MO	E(eV)	% of composition				
		Cl	H ₂ O	Benzimidazole	CH ₂ C ₆ (CH ₃) ₅	CH ₂ C(CH ₃)CH ₂
LUMO+5	− 0.35	0	0	5	75	20
LUMO+4	− 0.45	0	0	43	35	22
LUMO+3	− 0.73	0	0	59	10	30
LUMO+2	− 0.79	0	0	81	1	18
LUMO+1	− 1.10	0	0	98	2	0
LUMO	− 2.11	0	0	97	2	1
HOMO	− 5.73	94	1	2	2	1
HOMO-1	− 5.80	88	0	1	8	3
HOMO-2	− 5.92	86	7	6	1	0
HOMO-3	− 6.08	7	1	0	92	0
HOMO-4	− 6.30	1	0	0	99	0
HOMO-5	− 7.23	1	97	0	2	0
HOMO-6	− 7.52	1	0	3	0	96
HOMO-7	− 7.71	0	0	93	3	4
HOMO-8	− 7.82	0	0	96	1	2
HOMO-9	− 8.73	0	2	0	98	0
HOMO-10	− 8.79	0	0	2	98	0

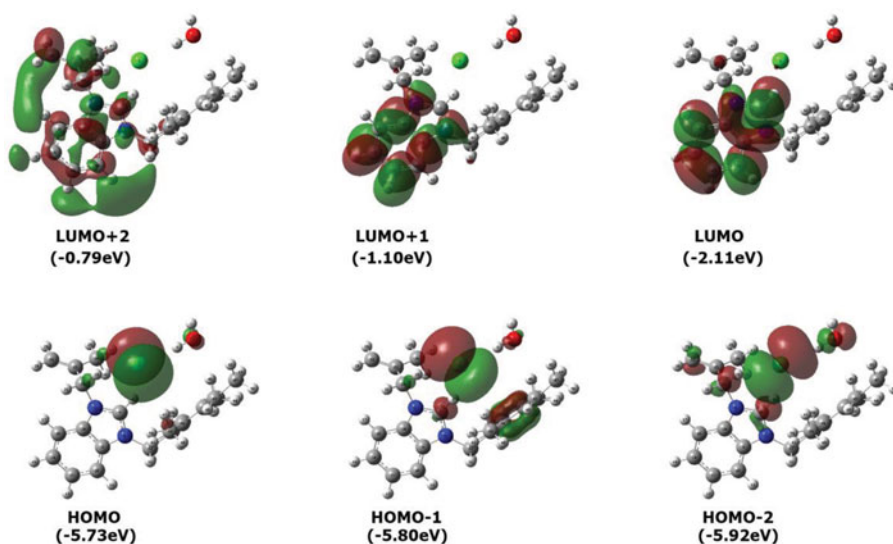


Figure 7. Contour plots of some molecular orbitals of **1**.

3.4. Mulliken and natural population analyses

Mulliken analysis that calculates the effective atomic charges is the most common population analysis. Mulliken charges are used to understand the charge distribution on the chemical bonding [48]. Atomic charges affect the electronic structure, dipole moment, molecular polarizability and more a lot of behavior of a molecular system. Atomic charges obtained by Mulliken population analysis and natural charges obtained by natural bond analysis for the title compound are listed in Table 8. The absolute values of the natural charges of all hydrogen atoms on the basis of NPA are normally positive. The absolute value of the natural charges is negative at all the heteroatoms in the molecule. The carbon atoms of pentamethylbenzyl are more negative when compare with the other aromatic carbons. This is in agreement with electrostatic potential lines (Fig. 8).

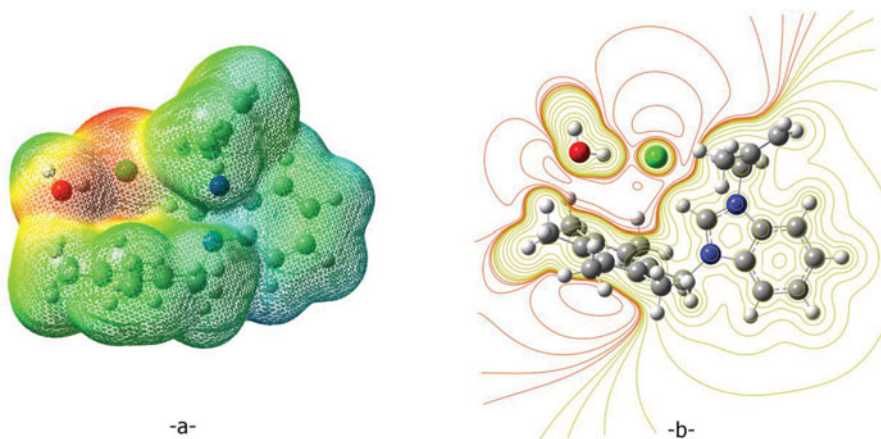


Figure 8. (a) Molecular electrostatic potential (MEP) of **1**. (b) Electrostatic potential (ESP) of **1**.

Table 8. Calculated net charges by Mulliken population method and natural population analysis.

Atom	6-311G++(d,p) Mulliken charges	6-311G++(d,p) Natural charges	Atom	6-311G++(d,p) Mulliken charges	6-311G++(d,p) Natural charges
Cl1	−0.517651	−0.87085	H1	0.422336	0.15277
O1	−0.558519	−0.97353	H3	0.169105	0.21330
H1A	0.181262	0.49422	H4	0.189067	0.21401
H1B	0.279651	0.45233	H5	0.190454	0.21435
N1	0.229462	−0.74069	H6	0.150379	0.22988
N2	0.316845	−0.45458	H8A	0.113408	0.28882
C1	−0.132473	0.94076	H8B	0.212031	0.20534
C2	0.318747	0.13054	H10A	0.133001	0.19476
C3	−0.156241	−0.68206	H10B	0.127290	0.18507
C4	−0.393997	−0.20293	H11A	0.170957	0.24394
C5	−0.449196	−0.18868	H11B	0.166468	0.20386
C6	−0.431361	−0.20501	H11C	0.165244	0.20974
C7	0.404731	0.14617	H12A	0.191248	0.21313
C8	−0.181266	−0.23361	H12B	0.220425	0.21951
C9	0.696892	−0.01444	H19A	0.181646	0.20960
C10	−0.627409	−0.37652	H19B	0.181033	0.24707
C11	−0.613020	−0.61297	H19C	0.124305	0.18629
C12	−0.593699	−0.17319	H20A	0.120872	0.20210
C13	0.351857	−0.10411	H20B	0.147297	0.20201
C14	0.359596	−0.00575	H20C	0.223423	0.25296
C15	0.426669	−0.01999	H21A	0.245834	0.19026
C16	0.262140	−0.13305	H21B	0.131167	−0.41727
C17	−0.102993	−0.04441	H21C	0.164091	0.06424
C18	0.489164	−0.02188	H22A	0.148966	0.20357
C19	−0.694650	−0.60134	H22B	0.203288	0.21344
C20	−0.836070	−0.62982	H22C	0.146868	0.21172
C21	−0.770930	0.32504	H23A	0.103162	0.19475
C22	−0.702662	−0.59875	H23B	0.193316	0.20849
C23	−0.813749	−0.59220	H23C	0.166863	0.21723

3.5. Electrostatic potential (ESP) and molecular electrostatic potential (MEP) analyses

ESP and MEP analyses of NHC salt **1** were performed by B3LYP/6-311G++(d,p) method at the 0.02 isovalues. Figure 8a,b shows the molecular electrostatic potential and contour of electrostatic potential for the title compound. The colour code of MEP map is in the range between the −7.352 a.u. (darkest red) and 7.352 a.u. (darkest blue), and potential increases in the order red < orange < yellow < green < blue.

The MEP mapped surfaces shows the charge distributions of molecules in three-dimensional and helps to determine the relative polarity of molecules and nucleophilic and electrophilic reactions [49, 50]. The contour maps are drawn in the molecular plain two dimensionally and used to show lines of constant density or brightness. The electron rich lines around oxygen and chlorine are theoretically potential active sides of the molecule and justify the intermolecular hydrogen bonding of NHC salt **1** as shown in the packing diagram. The green region shows the close to zero ESP value and characterize the C–C and C–N bonds.

4. Conclusion

Firstly, to obtain benzimidazole precursor, benzimidazole and 3-chloro-2-methyl-1-propene were reacted. Then, **1** was prepared and fully characterized by elemental analysis, X-ray crystallography, FT-IR, ¹H and ¹³C NMR spectroscopy techniques. In addition, the molecular geometry, vibrational frequencies and ¹H and ¹³C NMR chemical shift values of the compound have been calculated using DFT/B3LYP method. In the ¹H NMR spectrum of **1**, the signal for the acidic carbene proton at the 2-position in the benzimidazolium ring was observed

in the expected range. In the FT-IR spectrum, the characteristic bands assigned to the $\nu(\text{O-H})$ and $\nu(\text{C-H})$ vibrations of the compound were recorded in agreement with the previously reported results.

Although the discrepancies between the experimental and optimized geometric parameters, theoretical calculations support the solid state structure of **1**. This can mainly attributed to the solid state interactions in the crystal structure which are absent in the quantum mechanical modeling of the compound. The most negative potential areas in MEP are on oxygen and chlorine atoms and the X-ray analysis showed that these atoms act as acceptor in intra and intermolecular hydrogen bonding of compound. The electron rich lines around oxygen and chlorine in EPS are theoretically potential active sides of the molecule and verify the MEP map. Although the N atoms have high electronegativity, these atoms are concealed by high positive atoms in the region. The net charge distribution of title compound was calculated by the Mulliken and natural population methods. MEP, Mulliken population analysis, NPA results are consistent with each other related to chemically reactivity of molecule. The results of HOMO-LUMO and chemical reactivity analyses support the high electrical activity of the compound. The energy and compositions of some selected molecular orbitals were also calculated. The low energy unoccupied orbitals of the compound, from LUMO to LUMO+2, have π^* character and are concentrated on benzimidazole ring. The high energy occupied orbitals (HOMO—HOMO-2) of the compound have π character on Cl (p) orbitals. It would be helpful in next studies to understand the nature of electronic transitions in the compound.

Acknowledgements

The authors acknowledge the Scientific and Technological Research of Turkey (TÜBİTAK-BİDEB), the National Research Fellow-ship Programme for grants to N. Ş., Amasya University, Turkey, for the use of the Gaussian09W program and Ondokuz Mayıs University, Turkey, for the use of the STOE IPDS 2 diffractometer (purchased under grant F.279 of the University Research Fund).

Supplementary data

Crystallographic data for the structural analysis have been deposited with the Cambridge Crystallographic Data Center, CCDC reference number: 1582192. Copies of this information may be obtained free of the charge from the Director, CCDC, 12 Union Road, Cambridge, CB2 1EZ, UK (Fax: +44-1223-336033; E-mail: deposit@ccdc.cam.ac.uk or <http://www.ccd.cam.ac.uk>).

References

- [1] Wanzlick, H. W. & Schönherr, H. J. (1968). *Angew. Chem. Int. Ed.*, 7(2), 141.
- [2] Öfele, K. (1968). *J. Organomet. Chem.*, 12(3), 42.
- [3] Cardin, D. J., Çetinkaya, B., Lappert, M. F., Manojlović-Muir, L. & Muir, K. W. (1971). *J. Chem. Soc. D*, 8, 400.
- [4] Arduengo III, A. J., Harlow, R. L. & Kline, M. (1991). *J. Am. Chem. Soc.*, 113(1), 361.
- [5] Wanzlick, H. W. (1970). *Chem. Ber.*, 103(4), 1037.
- [6] Wanzlick, H. W. & Schönherr, H. J. (1970). *Liebigs Ann. Chem.*, 731, 176.
- [7] Walentowski, R. & Wanzlick, H. W. (1970). *Z. Naturforsch. B: Chem. Sci.*, 25(12), 1421.
- [8] Herrmann, W. A., Elison, M., Fischer, J., Köcher, C. & Artus, G. R. (1996). *Chem. Eur. J.*, 2(7), 772.
- [9] Herrmann, W. A., Köcher, C., Gooßen, L. & Artus, G. R. (1996). *Chem. Eur. J.*, 2(12), 1627.
- [10] Kuhn, N. & Kratz, T. (1993) *Synthesis*, 1993(06), 561.

- [11] Enders, D., Breuer, K., Raabe, G., Runsink, J., Teles, J. H., Melder, J. P., Ebel K. & Brode, S. (1995). *Angew. Chem. Int. Ed.*, 34(9), 1021.
- [12] Şahin, N., Demir, S. & Özdemir, İ. (2015). *Arkivoc*, 20.
- [13] Ortega, N., Tang, D. T. D., Urban, S., Zhao, D. & Glorius, F. (2013). *Angew. Chem. Int. Ed.*, 52(36), 9500.
- [14] Bortenschlager, M., Schütz, J., von Preysing, D., Nuyken, O., Herrmann, W. A. & Weberskirch, R. (2005). *J. Organomet. Chem.*, 690(24), 6233.
- [15] Van Rensburg, H., Tooze, R. P., Foster, D. F. & Slawin, A. M. (2004). *Inorg. Chem.*, 43(8), 2468.
- [16] Gürbüz, N., Karaca, E. Ö., Özdemir, İ. & Çetinkaya, B. (2015). *Turk. J. Chem.*, 39(6), 1115.
- [17] Godoy, F., Segarra, C., Poyatos, M. & Peris, E. (2011). *Organometallics*, 30(4), 684.
- [18] Paradiso, V., Bertolasi, V. & Grisi, F. (2014). *Organometallics*, 33(21), 5932.
- [19] Monsaert, S., De Canck, E., Drozdak, R., Van Der Voort, P., Verpoort, F., Martins, J. C. & Hendrickx, P. (2009). *Eur. J. Org. Chem.*, 2009(5), 655.
- [20] Munz, D., Allolio, C., Meyer, D., Micksch, M., Roessner, L. & Strassner, T. (2015). *J. Organomet. Chem.*, 794, 330.
- [21] Duan, W. L., Shi, M. & Rong, G. B. (2003). *Chem. Commun.*, (23), 2916.
- [22] Sakamoto, R., Morozumi, S., Yanagawa, Y., Toyama, M., Takayama, A., Kasuga, N. C. & Nomiya, K. (2016). *J. Inorg. Biochem.*, 163, 110.
- [23] Bertrand, B., Citta, A., Franken, I. L., Picquet, M., Folda, A., Scalcon, V., Rigobello, M. P., Gendre, P. L., Casini, A. & Bodio, E. (2015). *J. Biol. Inorg. Chem.*, 20(6), 1005.
- [24] Schmeier, T. J., Dobereiner, G. E., Crabtree, R. H. & Hazari, N. (2011). *J. Am. Chem. Soc.*, 133(24), 9274.
- [25] Riduan, S. N., Zhang, Y. & Ying, J. Y. (2009). *Angew. Chem. Int. Ed.*, 121(18), 3372.
- [26] Sanz, S., Benítez, M. & Peris, E. (2009). *Organometallics*, 29(1), 275.
- [27] Lee, C. H., Laitar, D. S., Mueller, P. & Sadighi, J. P. (2007). *J. Am. Chem. Soc.*, 129(45), 13802.
- [28] Sheldrick, G.M. (2015). *Acta Crystallogr. Sect. A*, 71, 3.
- [29] Sheldrick, G.M. (2015). *Acta Crystallogr. Sect. C*, 71, 3.
- [30] Spek, A. L. (2009). *Acta Crystallogr. Sect. D*, 65, 148.
- [31] Farrugia, L. J. (1999). *J. Appl. Crystallogr.*, 32, 837.
- [32] Frisch, M. J. et. al. (2009). *Gaussian 09, Revision E.01*, Gaussian Inc.: Wallingford, CT.
- [33] Andersson, M. P. & Uvdal, P. (2005). *J. Phys. Chem. A*, 109, 2937.
- [34] Wolinski, K., Hinton, J. F. & Pulay, P. (1990). *J. Am. Chem. Soc.*, 112, 8251.
- [35] Cancès, E., Mennucci, B. & Tomasi, J. (1997). *J. Chem. Phys.*, 107, 3032.
- [36] Liu, Q. X., Yin, L. N., Cheng, F. J., Guoa, J. H. & Songb, H. B. (2006). *Acta Crystallogr. Sect. E*, 62, 3604.
- [37] Korotkikh, N. I., Raenko, G. F., Pekhtereva, T. M., Shvaika, O. P., Cowley, A. H. & Jones, J. N. (2006). *Russ. J. Org. Chem.*, 42(12), 1822.
- [38] Özdemir, N., Dayan, O., Tercan Yavaşoğlu, M. & Çetinkaya, B. (2014). *Spectrochim. Acta, Part A*, 131, 145.
- [39] Akkoç, S., Kayser, V., İlhan, İ. Ö., Hibbs, D. E., Gök, Y., Williams, P. A., Hawkins, B. & Lai, F. (2017). *J. Organomet. Chem.*, 839, 98.
- [40] Durga, R., Anand, S., Rajkumar, K., Ramalingam, S. & Sundararajan, R. S. (2016). *J. Appl. Phys.*, 8, 01.
- [41] Bingöl Alpaslan, Y., Gökçe, H., Macit, M., Alpaslan, G. & Özdemir, N. (2015). *J. Mol. Struct.*, 1096, 43.
- [42] Doğan, Ö., Demir, S., Özdemir, İ. & Çetinkaya, B. (2011). *Appl. Organomet. Chem.*, 25(3), 163.
- [43] Eazhilarasi, G., Nagalakshmi, R. & Krishnakumar, V. (2008). *Spectrochim. Acta, Part A*, 71, 502.
- [44] Tanak, H., Alaman Agar, A. & Büyükgüngör, O. (2012). *Spectrochim. Acta, Part A*, 87, 15.
- [45] Demircioğlu, Z., Albayrak Kaştaş, Ç. & Büyükgüngör, O. (2015). *Spectrochim. Acta, Part A*, 139, 539.
- [46] Temel, E., Alaşalvar, C., Eserci, H. & Açar, E. (2017). *J. Mol. Struct.*, 1128, 5.
- [47] Xavier, R. J. & Dinesh, P. (2014). *Spectrochim. Acta, Part A*, 118, 999.

- [48] Arshad, M. N., Asiri, A. M., Alamry, K. A., Mahmood, T., Gilani, M. A., Ayub, K. & Biriniji, A. S. (2015). *Spectrochim. Acta, Part A*, 142, 364.
- [49] Saka, E. T., Uzun, S. & Çağlar, Y. (2016). *J. Organomet. Chem.*, 810, 25.
- [50] Dani, R. K., Bharty, M. K., Kushawaha, S. K., Prakash, O., Singh, R. K. & Singh, N. K. (2013). *Polyhedron*, 65, 31.